Integrated electro-optic Mach-Zehnder modulators based on Zn-diffused $LiNbO_3$ waveguides

G. Lifante (1), P.L. Pernas (2), E. Cantelar (1), F. Cussó (1) and I. Suárez (1)
1) Departamento de Física de Materiales, C-IV. Universidad Autónoma de Madrid. 28049-Madrid (Spain)
2) Departamento de Física Aplicada, C-XII. Universidad Autónoma de Madrid. 28049-Madrid (Spain)
email: gines.lifante@uam.es

Abstract
Integrated Mach-Zehnder modulators fabricated on X- and Z-cut lithium niobate wafers are presented. The optical waveguides were fabricated by the Zn-diffusion method, which allows monomode TM-propagation at the wavelength of interest by choosing the channel waveguide width. The TM-mode is shown to be buried beneath the surface, which avoids the need of using a dielectric buffer to reduce propagation losses induced by the metallic electrodes to perform electro-optic modulation. A figure of merit of 9.2 V·cm has been obtained for the switching voltage-interaction length product in Z-cut modulators with CCS configuration, which is slightly higher that the calculated theoretical value using the overlap between the externally applied electrical field and the propagating optical field.

Introduction
The integrated Mach-Zehnder intensity modulator is perhaps the paradigm of integrated optical devices, and it has been succesfully used in optics communications technology [1], and to perform other different tasks, such as for the fabrication of integrated Q-switched lasers [2]. Due to its high electrooptic coefficients, $LiNbO_3$ crystals have been widely used to implement integrated electrooptic Mach-Zehnder modulators, either using Ti-diffusion or proton exchange technologies for fabricating the optical circuits. Although these techniques give rise to high quality low loss channel waveguides, each of them present some drawbacks, such as the high temperature processing in the case of Ti-diffusion, or the fact that proton exchange waveguides only support extraordinary polarized propagating modes. Recently, Zn-diffusion has been considered an alternative approach for fabricating optical waveguides in $LiNbO_3$ [3], either by the evaporation of a ZnO layer over a $LiNbO_3$ substrate [4], or by the direct Zn incorporation on a $LiNbO_3$ substrate from its metallic vapor phase, both followed by a thermal annealing. In fact, Zn-diffusion technology has been used to developed some interesting integrated optical devices, including active devices on rare earth doped $LiNbO_3$ [5], as well as functional devices [4] based on the electro-optical properties of the $LiNbO_3$ substrates. In this work, electrooptic integrated Mach-Zehnder modulators on X- and Z-cut $LiNbO_3$ substrates fabricated by vapor Zn diffusion are presented, showing a versatile design and low half-wave voltages.

Mach-Zehnder fabrication
The general design of the integrated Mach-Zehnder interferometer is schematically shown in figure 1, where the electrodes have been positioned for the case of Z-cut substrates. The two symmetric Y-junctions (input and output) are implemented by two-opposed 2º arcs of circles with a high curvature radius of 20.5 mm, choosen to minimize losses in the bends [6]. The upper and lower parallel arms of the interferometer have a length of 11 mm, and are separated a distance of 50 μm. Considering the input and output straight channel waveguides, the the device has a total length of 2 cm. The input and output straight channel waveguides, as well as the two arms, have been fabricating using masks of either 2 or 4 μm. These designs are transferred by UV photolithographic techniques using SiO_2 intermediate stopping-masks 0.5 μm thick on X- and Z-cut congruent $LiNbO_3$ wafer supplied.

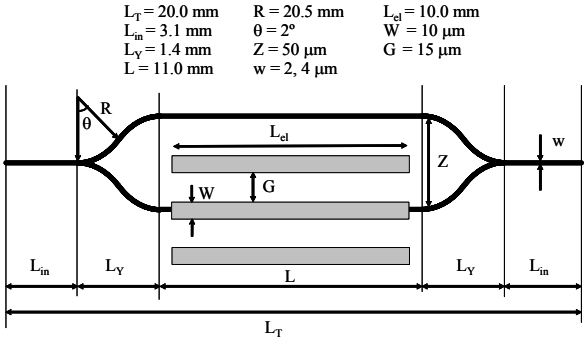

Fig.1. Integrated Mach-Zehnder interferometer design to fabricate electrooptic modulators. Electrodes are positioned for a Z-cut $LiNbO_3$ substrate.

After the lithography, waveguide fabrication was followed by the method described in reference [3], which consists on a vapor Zn diffusion at a temperature of 550 ºC during 2 hours followed by a thermal annealing in oxygen atmosphere: 850 ºC during 12 hours for the 2 μm channel width interferometer, and 900 ºC during 1 hour for the 4 μm wide channel waveguides. These parameters have been choosen to assure monomode behaviour at 1.55 μm wavelength. The optical characterization was performed by the end-fire-coupling technique at 0.633 μm and 1.55 μm, showing that the interferometers support both TE and TM propagation as expected, with a better guiding for TM polarization, and with no sign of

photorefractive damage even when using visible light. It has been also found that the extraordinary guides were buried some microns beneath the substrate surface, which can be the reason for the better guiding in this polarization as it has been discussed in [3]. The sizes of the fundamental modes for TM-propagation at 1.55 μm (measured at 1/e of the maximum) were 10.4x6.6 μm^2 and 10.6x7.3 μm^2, for the 2 μm and 4 μm wide channels, respectively, indicating some lateral diffusion of the Zn through the SiO_2 stopping mask during the annealing step.

Integrated electrooptic MZ modulators.

The next step in fabricating the integrated electrooptic modulators consists on depositing metallic electrodes along the arms of the interferometers. To use the highest electrooptic coefficient in $LiNbO_3$ (r_{33}), the externally applied electric field should be parallel to the Z-axis [7]. Therefore, in order to optimize the interaction between the electric field and the optical mode [8], in a Z-cut wafer the electrodes should be positioned on top of the waveguide arms (Fig. 2), while in an X-cut wafer the electrodes should be located on both sides of the branches. In these conditions the extraordinary index change by electro-optic effect in $LiNbO_3$ is given by [7]:

$$\Delta n_e = \frac{n_e \cdot r_{33}}{2} E_z \qquad (1)$$

where n_e is the extraordinary index, E_z the applied electric field and r_{33} the corresponding electro-optic coefficient (30.8 pm/V). As the r_{33} is three times higher that the r_{13} coefficient, the change on the ordinary index can be neglected. Following these considerations, the propagating light should be chosen TM-polarized in Z-cut substrates, and TE-polarized light when using X-cut wafers.

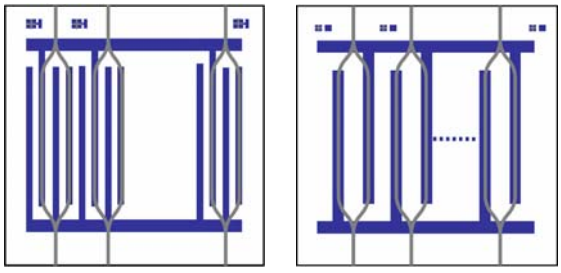

Fig. 2. Electrode mask alignement respect to the Mach-Zehnder interferometers on Z-cut substrates. Left: complementary coplanar stripline (CCS) Right: coplanar stripline (CS), forming a push-pull configuration. Note that the fourth electrode is initially not conected.

For Z-cut substrates the electrodes must be positioned on the top of the interferometric arms, while in X-cut substrates the electrodes lie besides the arms, in such a way that in both cases the major component of the electric field is along the crystal Z-axis. Also, the polarization chosen was the TM because it implies the higher electrooptic effect, and also it showed the better guiding as it has been discussed before.

Following this choice, 3000 Å thick and 10 μm wide aluminum electrodes were patterned by UV lithography on the position indicated in Figure 2, with a gap of 15 μm between electrodes and a length of 1 cm.

In other technologies, a buffer of SiO_2 must be placed between the waveguides and the metallic electrodes, in order to avoid the possible attenuation in the propagation mode. In our case, as the modes are buried some microns beneath the subtrate, the exponentially decay evanescent field of the mode does not reach the electrodes, and thus avoiding the need of using a dielectric intermediate buffer. Although the electrode mask was initially designed to work with Z-cut wafers, it is versatile enough to be used also with X-cut wafers, just by displacing laterally the electrode mask respect to the interferometer arms (see figure 3).

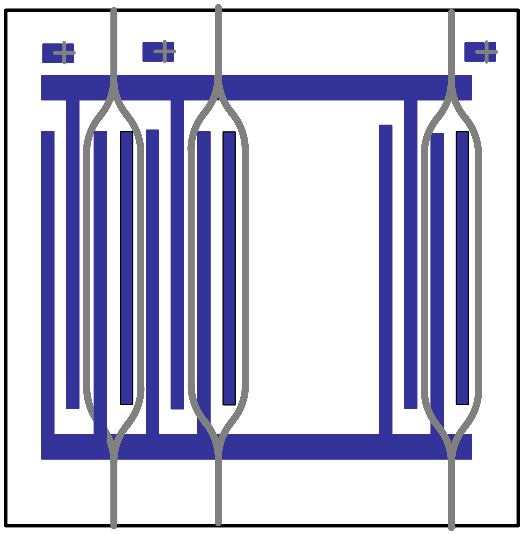

Fig. 3. Electrode mask alignement respect to the Mach-Zehnder interferometers on X-cut substrates. Let us note that the electrode mask is the same as that of figure 2 (left), showing the versatility of the mask design.

For this purpose, the electrode mask has several alignment motifs to be used for the different crystal cuts. Figure 4 shows an image of the left side of the EO-modulator, where it can be seen the channel waveguides, the metallic electrodes, as well as the alignement motifs.

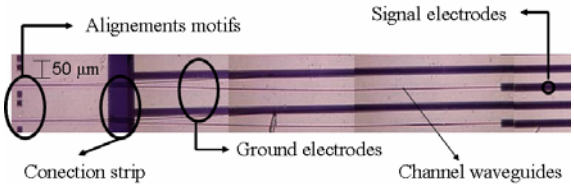

Fig. 4. Partial view of the integrated EO-modulator built into a Z-cut substrate.

The theoretical value for the half-wave voltage of the integrated electro-optic modulator can be calculated using the expression [9]:

$$V_\pi = \frac{\lambda\, g}{L\, n_e^3\, r_{33}\, \Gamma} \qquad (2)$$

where g is the gap between electrodes, L the electrode length and Γ a factor with relates the overlap between the applied electric field and the propagating modal field [10]:

$$\Gamma = \frac{\iint \varepsilon(x,y)\cdot E(x,y)\,dxdy}{\sqrt{\iint \varepsilon(x,y)^2\,dxdy}\cdot\sqrt{\iint E(x,y)^2\,dxdy}} \qquad (3)$$

where $\varepsilon(x,y)$ is the optical mode, and $E(x,y)$ the electric field produced by the metallic electrodes. Assuming an optical field intensity with dimensions of 10x9 μm^2 buried ~6 μm in the substrate and calculating the applied field with the mapping functions given in [7], an overlap factor of 0.48 is obtained. Using this value of Γ, and assuming that the electro-optic coefficient is not degraded by the Zn diffusion [4] a theoretical switching voltage of 6 volts is obtained for the configuration here designed.

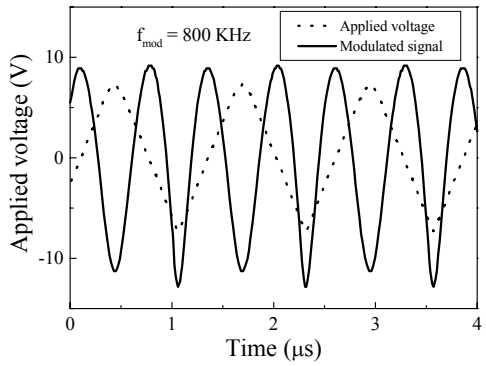

Fig. 5. Response of the integrated EO-modulator working at 800 KHz under a triangular electric signal, using a Z-cut substrate with CCS configuration.

To characterize the integrated electro-optic modulator, light from a polarized He-Ne laser is coupled into the interferometer input with the aid of a microscope objective, and a triangular wave coming from a HP-33120A wave-generator is applied to the modulator electrodes using gold wires. The modulated light at the interferometer output is collected and focused by means of a second microscope objective and detected by a S-20 photomultiplier ($\tau \sim 20$ ns). Both, applied voltage and modulated light intensity, were recorded by means of a 150 MHz digital oscilloscope Tektronics IX model TDS-420. Figure 5 shows the detected intensity (continuous line) when a triangular wave of 7.2 volts of amplitude (dashed line) is applied to the interferometer, at a frequency of 800 KHz. A plot of the modulated intensity versus the applied voltage gives the transfer function of the electro-optic modulator, where a half-wave voltage V_π of 9.2 V is obtained, and in consequence a voltage-length product of 9.2 V·cm, which is higher that the predicted theoretical value (6 V). This discrepancy between the theoretical and experimental V_π values can be attributed to an overestimation of the overlap factor given in equation (3).

Although no electro-optic modulation measurements have been taken at 1.55 μm, channel waveguides show monomode propagation at this wavelength when using a 2 μm width mask. The extrapolated half-wave voltage in this case using the relation (2) is 22.5 V, which is comparable with data reported by Twu et al. [4] using thermally evaporated Zn film to fabricate the channel waveguides, where they obtained a figure of merit of 9.6 V·cm using a push-pull MZ configuration, which reduces a half the switching-voltage.

The extintion ratios of the EO-modulators have been measured at 633 nm by comparing the maximum and minimum output intensity, using an oscilloscope working in DC mode. Figure 6 shows an example of these measurements, for a Z-cut modulator with CCS electrode structure, where a value of 7.6 dB has been obtained. Although this is not a very high value, it is expected that working at 1.55 μm the extintion ratio was superior, due to the monomode character of the channel waveguides at this wavelength.

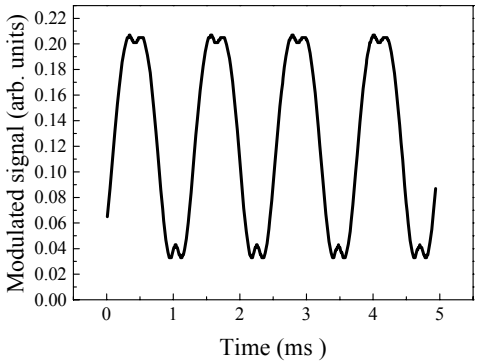

Fig. 6. Modulated signal, working on DC mode at the oscilloscope, for measuring the modulator extinction ratio.

Finally, the frequency response of the integrated EO-modulators has been obtained using the set-up previously described. Figure 7 shows the frequency behaviour, working under triangular wave, for 1 cm length electrode modulator. As it can be seen, the measured signal drops around 2 MHz. Unfortunately, this is the response limits of our measurement system (~20 ns), and thus this frequency represents a lower limit of the integrated EO-modulator. Theoretical estimations using the indicate a maximum frequency response of ~500 MHz

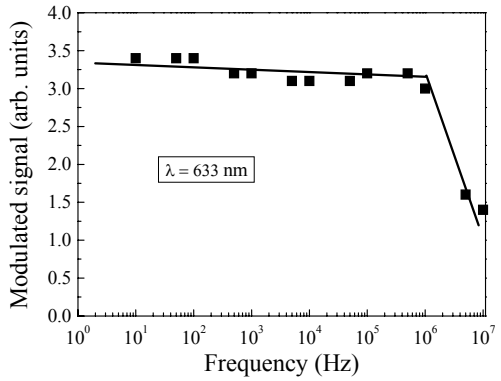

Fig. 7. Frequency response of the EO-modulator. The 2 MHz fall is just the limit of the measurement set-up, and thus indicates a lower limit for the frequency response of the modulator.

Conclusions

Integrated electro-optic modulators fabricated by the vapour Zn diffusion method in $LiNbO_3$ have been demonstrated. The design of the interferometric and electrodes masks is versatile in the sense that they can be used for X-cut wafers, just by shifting the electrodes respect to the waveguides. Also, the Zn diffusion technique for fabricating n_e guides has the advantage of avoiding the need of using a buffer to reduce propagation losses, as it is needed when using Ti diffusion technique. The electro-optic modulator shows a figure of merit of 9.2 V·cm, which is a little higher than the theoretical value, probably due to an overestimation of the overlap factor.

Acknowledgments

This work has been partially supported by the Ministerio de Ciencia y Tecnología and Comunidad de Madrid (Spain) under projects MOISES (MAT2005-05950) and MICROSERES (GR-MAT-0108-2004).
The authors acknowledge the technical support provided by Prof. W. Sohler group in the infrared interferometer characterization.

References

[1] K. Noguchi et al, Electronics Letters 28, p. 1759, 1992
[2] H. Suche et al, Electronics Letters 34, p. 1228, 1998
[3] I. Suárez et al, Optical Materials, 2006 (submitted).
[4] R. Twu et al, Microwave and Optical Technology Letters 43, p. 142, 2004.
[5] E. Cantelar et al, Applied Physics Letters 86, p. 161119, 2005
[6] L. Lerner, Electronics Letters 29, p. 733, 1993
[7] Ed. L. Wooten et al, IEEE J. Select. Topics in Quantum Electron. 6, p. 69, 2005
[8] O.G. Ramer, IEEE J. of Quantum Electron., 18, p. 386, 1981
[9] R.C. Alferness, IEEE Transactions on Microwave Theory and Techniques 30, p. 1121, 1982